Project Number: JDV – 1002

Multi-Actuator Switch-Mode Hydraulic System

A Major Qualifying Project Report

Submitted to the Faculty

of

Worcester Polytechnic Institute

in Partial Fulfillment of the Requirements for the

Degree of Bachelor of Science

By

_____

Patrick Ennis

_____

Peter Forte

_____

Brendan Gove

_____

Christopher Wellington

Date: April 28, 2011

Approved:

_____

Professor James D. Van de Ven

Abstract

Current hydraulic systems involving multiple actuators and a single hydraulic power supply generally have poor efficiency. Using throttling valves to control multiple actuators requires meeting the highest pressure requirement and the total flow of all of actuators. When there is a large difference in the pressure requirement of the actuators, fluid throttling results in significant energy losses. The purpose of this project is to implement switch-mode control in a multi-actuator circuit and demonstrate the improvement in efficiency over a traditional hydraulic system with throttling valve control. To accomplish this task a hydraulic crane arm powered by two actuators was designed and constructed. One actuator provides a pivoting motion utilizing low pressure and high flow, while the other provides a lifting motion utilizing high pressure and low flow. Using a simple feedback control loop, the crane arm lifts, rotates, and lower a load. After designing and testing the hydraulic crane, the team concluded that high-speed switch technology with multiple actuators is feasible. This new technology, once implemented on a larger scale in realistic applications, will reduce losses in hydraulic systems that depend on multiple actuators to function.

Table of Contents

Table of Figures

Introduction

Throttling Systems

The concept of fluid power has many applications ranging from high precision robotics to critical systems in the vehicles that many rely on every day. The basic purpose of a fluid power circuit is to convert mechanical energy into fluid energy. Once this conversion is made, the system must deliver the power to where it is needed in the system and convert the fluid energy back into mechanical energy. In many cases, it is possible to achieve the desired end result without any conversion to fluid energy. When the energy needs to be delivered to a location far away from the energy source, however, a complex system of gears, chains, belts, and linkages would be necessary. This often comes at the expense of the cost, simplicity, and reliability of the system. A typical fluid power circuit is comprised of a hydraulic pump, to convert mechanical energy to fluid energy, a series of hoses to carry the fluid to its required location, and an actuator to convert the fluid energy back into mechanical energy. The remainder of the system is comprised of simple and generally inexpensive control components, such as valves and accumulators. The chief advantage of fluid power is its ability to deliver substantial amounts of energy to remote locations without the need for cumbersome mechanisms.

This ability to deliver energy to a remote location comes at the price of efficiency. In *Fluid Power Circuits and Controls*, Cundiff (1) lays out a simple example of a hydraulic circuit used to lift a mass with a linear actuator. In his analysis, Cundiff accounts for pressure drops in hydraulic lines and across valves in the system. He demonstrates that these losses require the pump to provide a 23% higher pressure than it would in a system without losses. Compared with a simple single reduction gear box which operates at 98-99% efficiency, a hydraulic system performing the same task has a relatively poor efficiency. Furthermore, typical pumps convert between mechanical and fluid energy at roughly 85% efficiency. Because any hydraulic circuit will need to do this conversion twice, once at the energy source and once at the application, this results in an efficiency of only 72%. When these conversion losses are combined with the losses due to pressure drops within the system, it becomes clear that fluid power circuits provide poor efficiencies compared to their mechanical system counter parts.

The problem of inefficiency is further compounded when one starts to consider real applications of hydraulic circuits. In many cases, it is desirable to control multiple actuators with a single hydraulic circuit. Vehicle wheels driven by hydraulic motors are a good example of this concept. To accomplish tasks such as turning and traction control, each actuator needs to be provided with varying pressures and flows depending on the torque and angular velocity requirements of that wheel at a particular time. Another example of a multi-actuator application is a two degree of freedom crane arm whose lifting and rotating motions are controlled by separate actuators. The conventional design of a hydraulic circuit for one of these applications would use a single hydraulic pump with throttling valves to control the pressures and flows each actuator receives. Throttling control is inherently inefficient.

Consider the example of a crane arm used to lift and rotate a load. In this case, the actuator responsible for lifting the load would typically require a high pressure, but a relatively low flow rate. With the force an actuator provides being directly proportional to the pressure behind its cylinder, higher pressures are required to lift larger loads. In the interest of reducing the power required for the lift, lower flow rates are typically used for high loads. For the rotation, however, a much lower force is required but a higher flow rate is desired to move the load more quickly. Both of these actuators are being powered by the same pump, which needs to provide sufficient pressures and flows to meet the requirements of the high pressure actuator as well as the sum of flow requirements of the actuators. As shown in Figure 1, Van de Ven (2) illustrates the difference in energy provided by the pump and the energy used by the actuators for a typical system with three actuators.

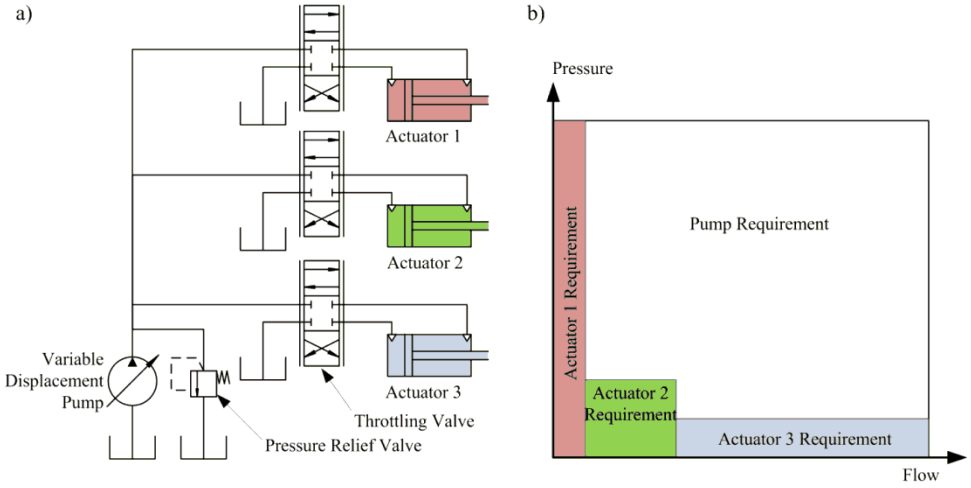

Figure 1: a) Throttling Schematic b) Pressure vs. Flow plot

As seen in Figure 1, actuator 1 requires a high pressure and a low flow rate. Actuator 2 requires moderate pressure and moderate flow rate. Actuator 3 requires low pressure and a high flow rate. Power is the product of pressure and flow. Therefore, areas in this plot represent the power provided by the pump and the power required by each actuator. The necessary power from the pump greatly exceeds the power requirements of each actuator, resulting in a substantial loss of energy in the system. Efficiency, therefore, is of great concern when one considers line losses, pump losses, and losses due to multiple actuators with varying pressure requirements in a hydraulic system

An alternative method that improves efficiency is the use of a variable displacement pump. The variable displacement pump works by using pistons aligned in a barrel that is spun by an engine, rotating the pistons uniformly. The pistons then extend out of the barrel and are connected to a swash plate. As the angle of the swash plate changes, the pistons are forced out of the barrel and oil is brought into the cylinder from the tank. The swash plate is held stationary while the barrel with pistons rotates, pumping oil into the system. By changing the angle of the swash plate, the amount of oil that is pumped into the system changes. The larger the angle, the more oil is pumped through the system. This angle is set to the needs of the hydraulic system shown below in Figure 2.

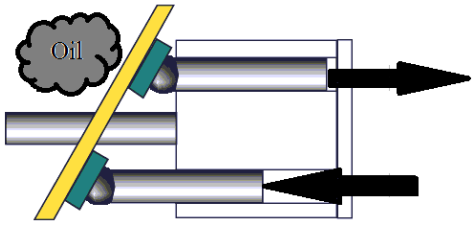

Figure 2: Cylinder Action (3)

A load sensing hydraulic system adjusts the angle of the swash plate and hence the amount of oil in the system. The variable displacement pump is more efficient than a fixed displacement pump because it pumps only what the system needs. When the system does not require fluid, the pump stops running, lowering the fuel consumption of the device. These pumps have their own drawbacks: they are expensive, complicated, and bulky. These drawbacks make variable displacement pumps a poor choice for most applications.

Switch-Mode Control

A new technology called switch-mode control provides a more energy efficient alternative to throttling valve control. This method of control uses a high speed valve to rapidly switch an actuator on and off. The valve is turned on and off at a constant frequency. Its duty cycle, defined as the ratio of on time to the switching period, is varied according to the pressure requirements of the actuator to achieve the desired result. Higher pressure requirements are satisfied by higher duty cycles. When this basic technology is applied to multi-actuator circuits, the energy savings become substantial.

Consider again the example of a crane lifting and rotating a load. When this circuit is controlled by high speed on/off valves, the pump still needs to provide pressures equal to or slightly exceeding the maximum pressure required by the lifting actuator. The flow requirements of the pump are far lower than in the throttling valve controlled alternative. To provide the high pressure for lifting, the duty cycle of the lifting valve is set to close to 100%, providing nearly 100% of the pressure output of the pump, with nearly 100% of the flow coming from the pump.

For the rotation, however, a much lower pressure is needed. If the pressure requirement of this actuator is 20% of the pump pressure, the duty cycle of the valve for this branch of the circuit would be set to 20%. With flow coming from the pump for 20% of the cycle and from the tank for the remaining 80%, the addition of a second actuator in the circuit only increases the flow requirement of the pump a small amount compared to a circuit controlled by throttling. In the conventional throttling configuration, the entire flow requirement for each actuator must be provided by the pump continuously. Figure 3 below shows a schematic of a typical switch-mode controlled hydraulic circuit and demonstrates the reduced pump requirement using pulse-width modulated signal control.

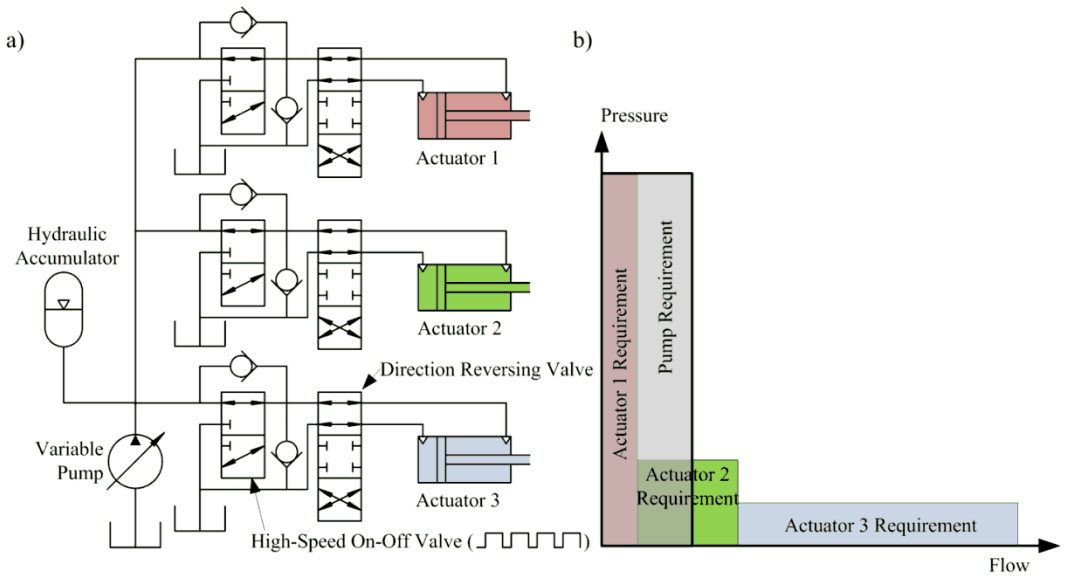

Figure 3: a) Switch-Mode Schematic b) Switch-Mode Pump Requirement

The application of switch-mode control to multi-actuator hydraulic circuits shows great promise of improved efficiencies. Due to the physical limitations of conventional on/off valve designs, commercially available valves are typically only capable of frequencies of 10 Hz. A phase-shift high speed valve is currently being developed to address this frequency limitation (4). This design uses a valve plate which rotates with a constant angular velocity between two port plates. Duty cycle control is accomplished by varying the orientation of the port plates relative to each other. The valve plates avoid switching by linear actuation, giving this design the potential to provide significantly higher frequencies than commercially available valves. The primary benefits of this new technology are a higher switching frequency and a smoother operation of the system.

The final advantage of a switch-mode control system is the ability to use an accumulator for energy regeneration in the hydraulic circuit. The accumulator is initially pressurized by a conventional variable displacement pump. The ability of a hydraulic system to re-capture the energy put into the system using the decelerating motion of the system to re-pressurize the accumulator increases the efficiency of the system significantly.

The purpose of this project was to implement switch-mode control in a multi-actuator circuit and demonstrate the improvement in this system's efficiency over a traditional hydraulic system. The constructed system mimics a crane arm lifting and rotating a load. Mathematical models of the dynamic forces and stresses in the device were developed to aid in the design of

the crane arm, discussed in the Mechanical Crane Arm Design section. These calculations were also used to properly size the hydraulic circuit, as covered in the Design of Hydraulic Circuit section. An electronic circuit and a software program called LabVIEW were used to power and control the physical components of the system, discussed in the Design of the Control System section. The team used this system to gain insight into the behavior of switch-mode hydraulics. Based on the results, the team discussed the feasibility of implementing switch-mode hydraulics on a large scale, and drew conclusions about the future of this innovative hydraulic technology.

Methods

Background Research

In order to implement switch-mode control in a multi-actuator circuit, a mechanism was needed for the hydraulic circuit to control. Two potential applications were considered at the outset of the project. The first was a test stand that would simulate the power train of a hydraulic hybrid vehicle. This would incorporate hydraulic motors to drive multiple wheels, as in a vehicle powered by hydraulics. Different pressure and flow requirements would simulate high speed and low torque, or low speed and high torque situations.

The other option was to design a crane arm. This application was a much simpler mechanism with the two degrees of freedom required to demonstrate the switch-mode control. Due to the fact that the purpose and focus of the project was to implement switch-mode control in a multi-actuator circuit and demonstrate the improvement in efficiency, the simple crane arm application was the most logical choice.

Goal Statement

To construct a two-degree of freedom crane arm powered by a switch-mode controlled multi-actuator hydraulic circuit.

Task Specifications

1. Mechanism must have a natural frequency at least twice the driving frequency of 10 Hz
2. Mechanism must be able to withstand operational vibrations
3. Mechanism must have two degrees of freedom – one high pressure low flow, one low pressure high flow
4. Mechanism must be able to support mass of 50 lbs.
5. Mechanism must be able to rotate 90°
6. Hydraulic pump must be powered by 110 VAC
7. The system must operate in the range of 0 - 3000 psi
8. System noise should not exceed 75 dB
9. System must fit on a 3.5’ x 2.25’ Festo mounting board
10. Mechanism must be able to lift through an angle of 20°
11. Cost of all components must not exceed $1,500

Mechanical Crane Arm Design

As an application for a multi-actuator switch-mode controlled hydraulic circuit, a small scale crane arm mechanism was designed to lift a 50 lb. dumbbell. The mechanism has two degrees of freedom which simulate a crane lifting and rotating a load. This application fits well with the switch-mode hydraulic circuit as the cylinder that lifts the mechanism requires high pressure and low flow, while the cylinder that rotates the mechanism requires low pressure and high flow. The group iterated through several preliminary designs and performed an analysis of the stresses, deflections, and natural frequencies on the final design to ensure its ability to withstand the forces in the system.

The preliminary mechanism design incorporates a central housing containing ball bearings which allow the shaft to rotate about a fixed axis. The arm and hydraulic cylinders are then connected to the housing with a set of brackets. This configuration, shown in Figure 4 below, allows the mechanism to lift and rotate independently.

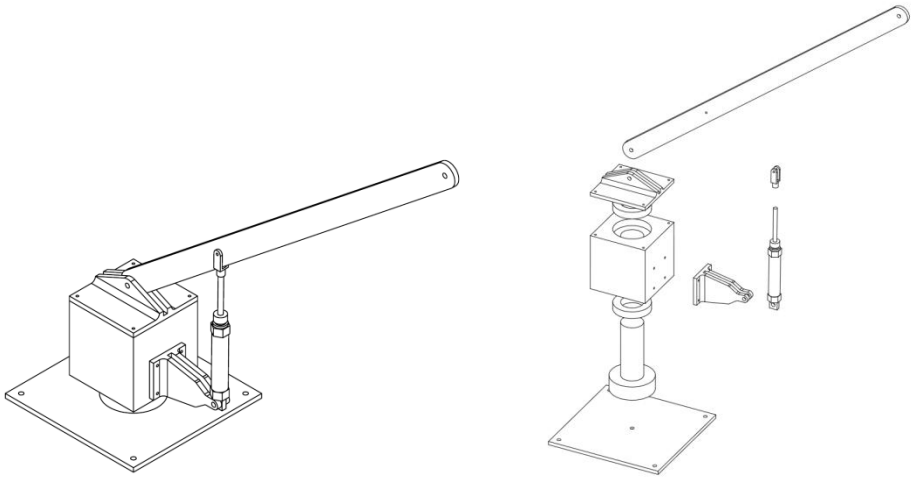

Figure 4: Preliminary Mechanism Design

Several improvements were made to the mechanism before true detailed design and analysis began. First, the solid rectangular bar used for the arm was replaced with hollow square tubing. Square tubing provides stiffness in both horizontal and vertical directions, ensuring the arm does not flex during the lifting or rotating motions. Additionally, the housing was modified to reduce the number of required brackets. Instead of bolting a separate bracket onto the top of the housing to support the arm, a U-shaped channel was cut into the top of the housing block.

The arm rests in this channel, with a pin passing through the housing and arm to serve as a pivot. This change eliminated a welded part from the design, as well as four fasteners and tapped holes, simplifying the manufacturing of the mechanism considerably.

The design of the main shaft was also improved in several ways. In the preliminary design, shown in Figure 4, the shaft is a single solid piece stepped down to provide a base for mounting and a shoulder for the lower bearing to rest against. This design was undesirable because machining it from a single piece of bar stock would require removing a considerable amount of material. One potential solution was to weld the larger diameter round plate to the bottom of the shaft stock. This would eliminate excess machining, but posed the problem of heat from the welding operation distorting the vertical alignment of the shaft.

In the final design of the main shaft, the problems associated with welding and stepping down a larger diameter shaft were both avoided. In this design, shown in Figure 5, precision-ground shaft stock is attached to a base plate with a socket head cap screw. The cap screw sandwiches a washer between the base plate and the bottom of the shaft, providing the necessary shelf for the inner race of the lower bearing. At the top of the shaft, the diameter is turned down to accommodate external threads. These threads allow two jam nuts to provide a preload on the ball bearings, locking the housing in place vertically, but still allowing it to rotate about the shaft.

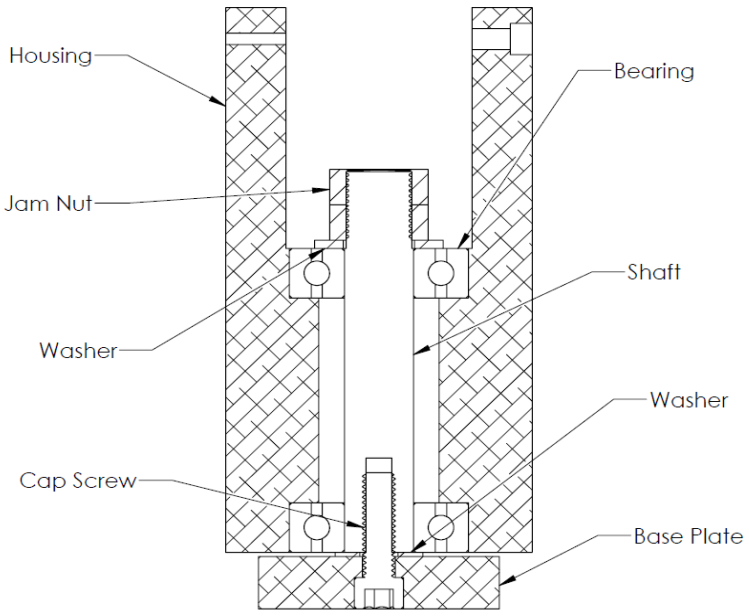

Figure 5: Modified Shaft Assembly

Dynamic Force Analysis

After settling on a practical design concept for the arm and housing assemblies, detailed design was completed for each component of the mechanism. In order to properly size each component, a kinematic and dynamic analysis of the motions of the mechanism was performed. This analysis provided information about the loads on each component, which was then used to determine stresses, deflections, and natural frequencies as appropriate.

The first step in the kinematic analysis of the mechanism was specifying the desired motion for the lift and rotation of the mechanism. To ensure a smooth trajectory with zero velocity and acceleration at the beginning and end of each motion 3-4-5 polynomial functions, most widely used for cam design applications, were used to specify the position of each hydraulic actuator at a given point in time. The general form of the 3-4-5 polynomial displacement function, equation 8.24 in Norton's *Design of Machinery* (5) is as follows:

$$s = h\left[10\left(\frac{\theta}{\beta}\right)^3 - 15\left(\frac{\theta}{\beta}\right)^4 + 6\left(\frac{\theta}{\beta}\right)^5\right] \qquad \text{Eqn. (1)}$$

For the case of an actuator extending over time, the ratio $\frac{\theta}{\beta}$ was replaced with $\frac{t}{t_{tot}}$, where t is the current time and t_{tot} is the total actuator extension time. For a given actuator, h is the stroke length, and s is the displacement at time t, starting at zero and ending at the stroke length. For the kinematic analysis of the arm mechanism, it was desirable to have an expression for the total length of each actuator with respect to time. To obtain this expression, the initial length of each actuator, s_0 was added to their displacement functions. The complete expression defining the total length of each actuator is as follows:

$$s = h\left[10\left(\frac{t}{t_{tot}}\right)^3 - 15\left(\frac{t}{t_{tot}}\right)^4 + 6\left(\frac{t}{t_{tot}}\right)^5\right] + s_0 \qquad \text{Eqn. (2)}$$

This expression and its first three derivatives define the SVAJ diagrams shown below in Figure 6. The lifting actuator, shown on the left, has an initial length of 8.3125 inches, stroke of two inches, and total time of five seconds. The rotating actuator, shown on the right, has an initial length of 8.5625 inches, stroke of four inches, and total time of two seconds. These combinations of stroke length and total time were chosen to give the lifting actuator a relatively low flow in comparison with the rotating actuator's high flow. Note that in both cases, velocity

and acceleration are zero at the start and end of the motions, and jerk is finite throughout. These conditions ensure smooth motion of both actuators.

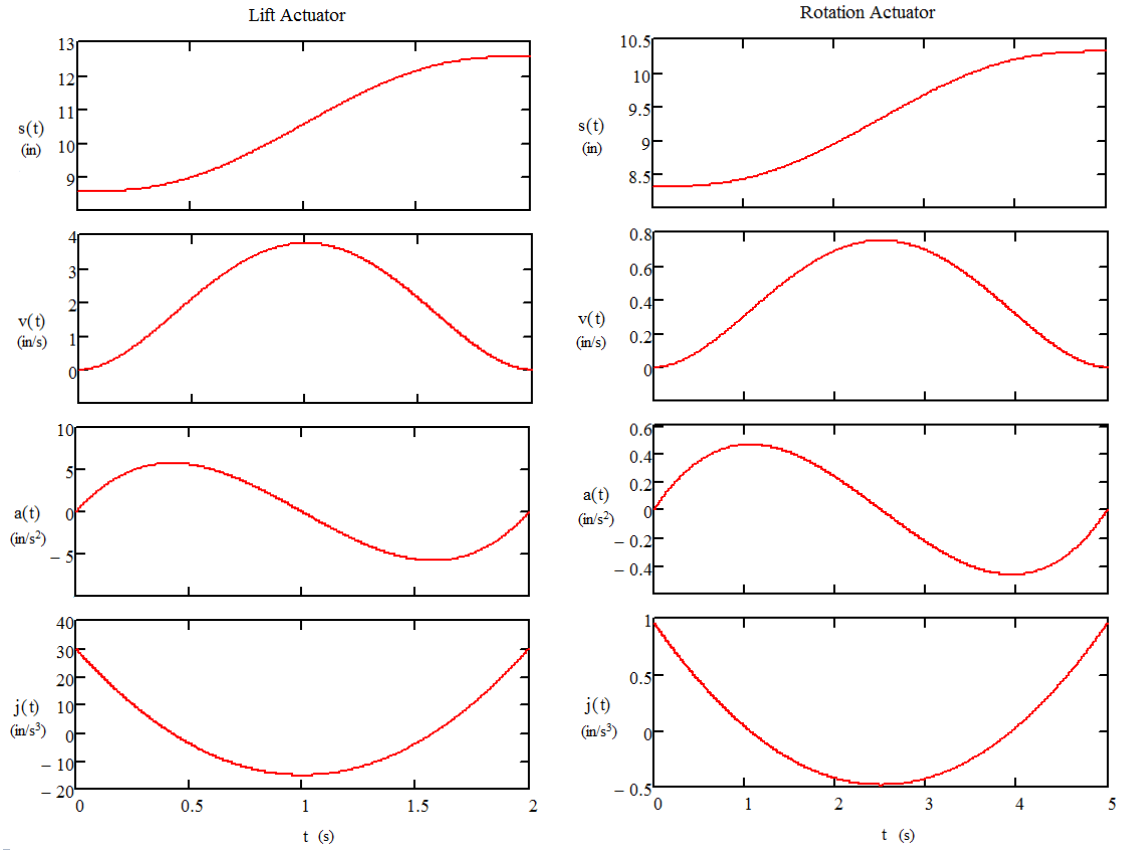

Figure 6: Lift and Rotation SVAJ Diagrams

With the lift and rotation kinematics defined, a dynamic analysis was performed to determine the inertial and gravitational forces applied at the end of the arm and the resulting forces in each actuator necessary to induce the desired motion. First, the geometry of the lifting mechanism was defined. Figure 7 below serves as a key to define all the necessary geometric variables in the system.

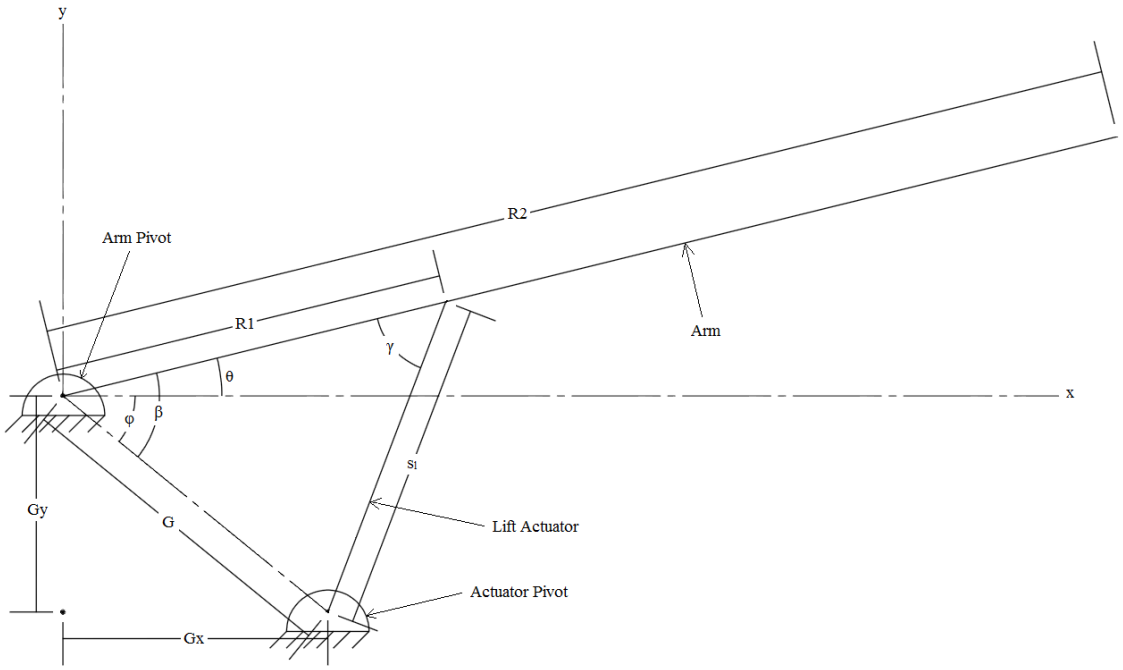

Figure 7: Lift Variable Key

In Figure 7, *R1*, *R2*, *Gx*, and *Gy* are fixed values. The value s_l is the length of the lifting actuator, defined above with the 3-4-5 polynomial function. The angles θ, β, and γ vary with the length of the actuator. The value of γ is defined as follows using the law of cosines:

$$\gamma = \cos^{-1}\left(\frac{R1^2 + s^2 - G^2}{2 * R1 * s_l}\right) \qquad \text{Eqn. (3)}$$

The value of β is defined as follows using the law of sines:

$$\beta = \sin^{-1}\left(\frac{s * \sin\gamma}{G}\right) \qquad \text{Eqn. (4)}$$

The value of θ is simply:

$$\theta = \beta - \varphi \qquad \text{Eqn. (5)}$$

The expression for θ was differentiated twice with respect to time to attain an expression for the angular acceleration of the arm over the five second lift period. Figure 8 below shows a plot of the angular acceleration of the arm, in $\frac{radians}{s^2}$. As expected, the angular acceleration is zero at the start and end of the motion, is positive for the first half, and negative for the second half of the cycle.

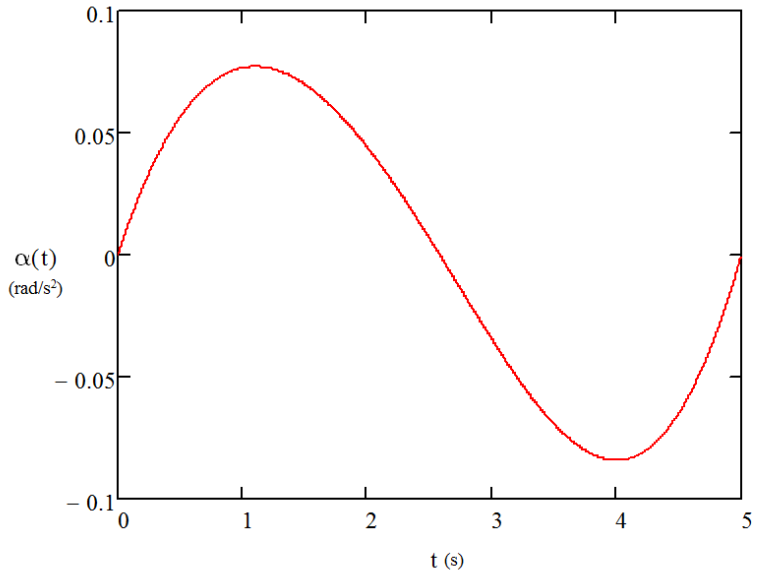

Figure 8: Lift Angular Acceleration

The angular acceleration of the arm was then used to determine the kinetostatic, or inertial force on the arm due to the accelerating load. The arm-mass system was treated as a point mass *m* at a radius equal to the arm's length, *R2*. This system has a mass moment of inertia, *I* as follows:

$$I = m * R2^2 \qquad \text{Eqn. (6)}$$

The inertial torque is given by Newton's law as follows:

$$T = I * \alpha = m * R2^2 * \alpha \qquad \text{Eqn. (7)}$$

Dividing by the length of the arm gives the tangential kinetostatic force applied to the end of the arm due to the accelerating mass:

$$F_k = m * g * R2 * \alpha \qquad \text{Eqn. (8)}$$

This inertial force, F_k, combines with the component of the gravitational force normal to the arm to represent the total load which puts the arm in bending. There is also a component of the gravitational force parallel to the arm which compresses the arm axially. Figure 9 below shows a plot of the total tangential force experienced by the arm during its five second lift.

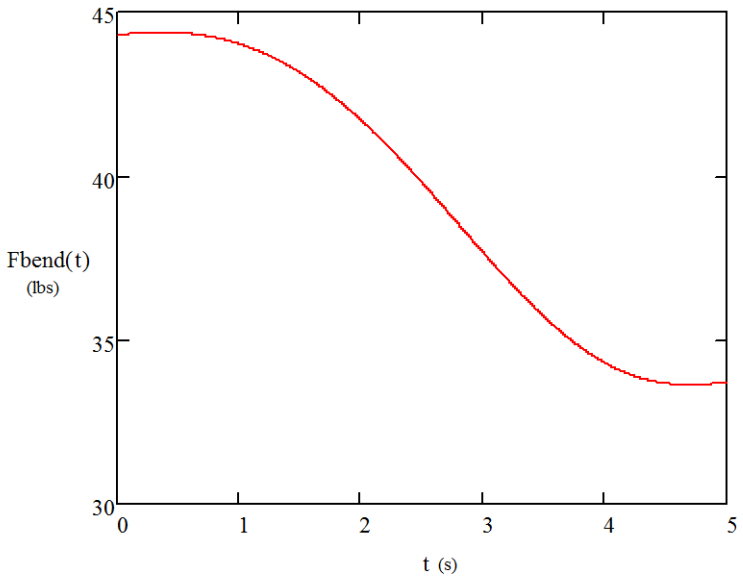

Figure 9: Normal Bending Force During Lift

This function has a maximum value of 44.37 lbs, which was used to calculate the maximum stress and deflection of the arm during the lift. The arm was treated as a beam with two pin supports and an overhung load. The free body diagram for this case is shown below in Figure 10.

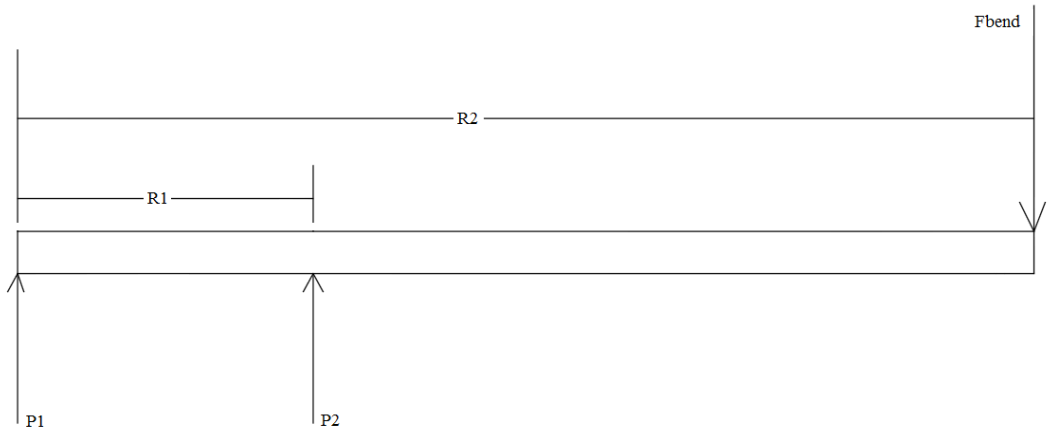

Figure 10: Free Body Diagram of Arm

Singularity functions were used to define the load, shear, moment, slope, and deflection functions for the beam. These functions are as follows:

$$q = P1\langle x - 0\rangle^{-1} + P2\langle x - R1\rangle^{-1} - Fbend\langle x - R2\rangle^{-1} \qquad \text{Eqn. (9)}$$

$$V = P1\langle x-0\rangle^0 + P2\langle x-R1\rangle^0 - Fbend\langle x-R2\rangle^0 \qquad \text{Eqn. (10)}$$

$$M = P1\langle x-0\rangle^1 + P2\langle x-R1\rangle^1 - Fbend\langle x-R2\rangle^1 \qquad \text{Eqn. (11)}$$

$$\theta = \frac{1}{EI}\left[\frac{P1}{2}\langle x-0\rangle^2 + \frac{P2}{2}\langle x-R1\rangle^2 - \frac{Fbend}{2}\langle x-R2\rangle^2\right] \qquad \text{Eqn. (12)}$$

$$y = \frac{1}{EI}\left[\frac{P1}{6}\langle x-0\rangle^3 + \frac{P2}{6}\langle x-R1\rangle^3 - \frac{Fbend}{6}\langle x-R2\rangle^3\right] \qquad \text{Eqn. (13)}$$

The pin reaction forces, *P1* and *P2* were calculated by summing the forces and moments on the arm. For *Fbend* equal to 44.37 lbs, *R1* equal to seven inches, and *R2* equal to 18 inches, *P1* equals -69.7 lbs and *P2* equals 114.1 lbs. For this load and reaction forces, the shear and moment diagrams for the arm are shown below in Figures 11 and 12:

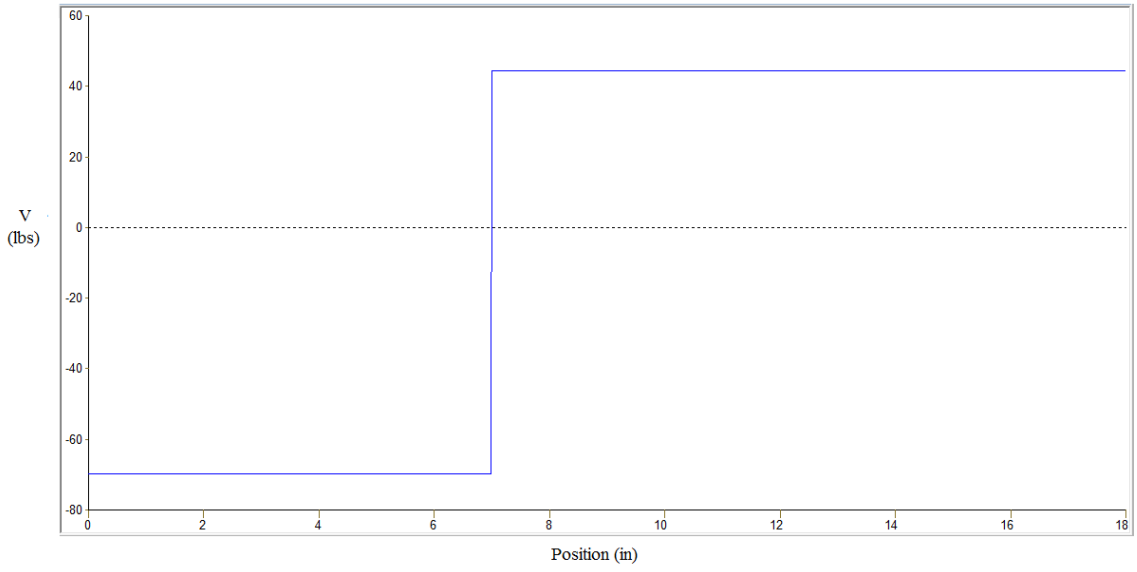

Figure 11: Shear Diagram

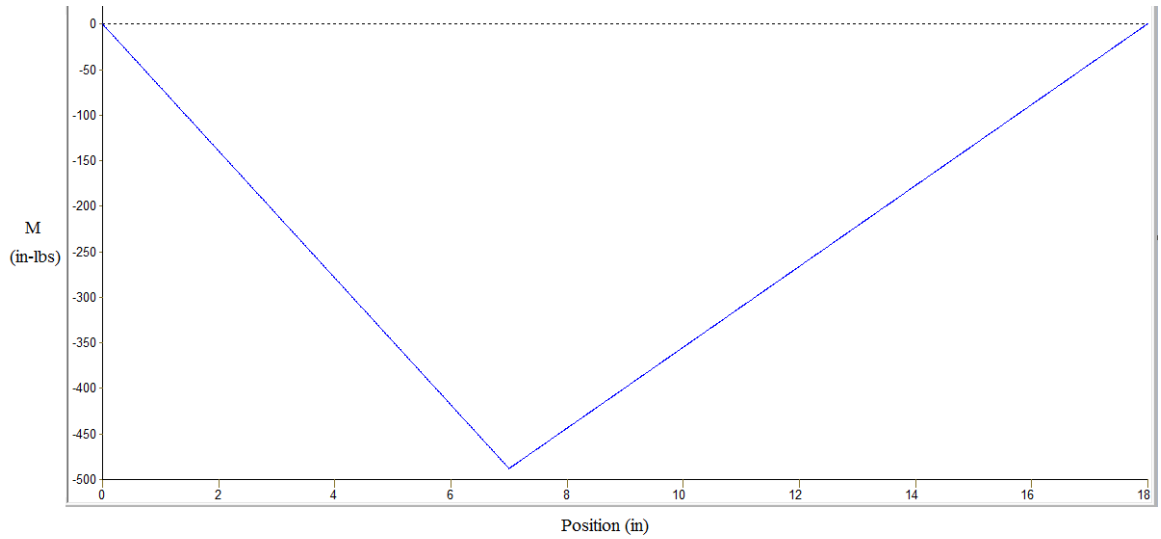

Figure 12: Moment Diagram

The moment diagram indicates a maximum bending moment of 487.9 in-lbs. at an x-position of seven inches, the point where the actuator attaches to the arm. The maximum bending stress, which occurs at the arm's outer fibers, is given by the flexure formula:

$$\sigma_{max} = \frac{Mc}{I} \qquad \text{Eqn. (14)}$$

Where *M* is the bending moment, *c* is the distance from the beam's neutral axis to the outer fiber, and *I* is the area moment of inertia. Since *c* and *I* both depend on the arm's geometry, a commercially available square tubing size was chosen and the maximum stress was calculated for this size. 2" x 2" x $\frac{1}{8}$" wall thickness 6061 aluminum tubing was chosen for the arm. This cross-section has a *c* value of one inch and *I* value of 0.552 inches^4. This gives a maximum bending stress of 884 psi.

This bending stress combines with the axial tension and compression due to the axial component of the gravitational force on the load. To determine this axial load, it was first necessary to determine the force generated in the actuator and the total force in the main pivot pin. The force which must be generated in the actuator to provide the normal force necessary for the lift can be expressed as follows:

$$F_{act} = \frac{F_{act,normal}}{\sin\gamma} \qquad \text{Eqn. (15)}$$

This force is important later on for proper sizing of the hydraulic circuit, so its value over the five second lift time is plotted in Figure 13 below:

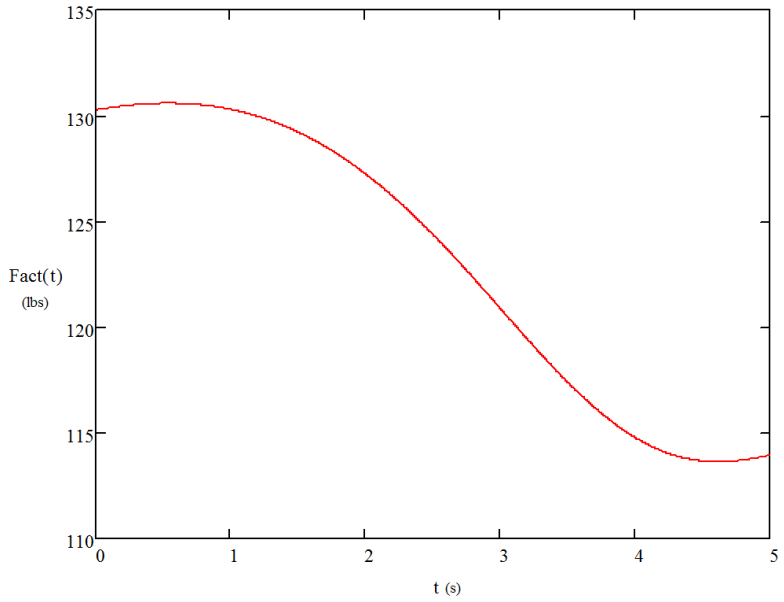

Figure 13: Lift Actuator Force

The component of this force parallel to the arm is given as follows:

$$F_{act,parallel} = F_{act} * \cos\gamma \qquad \text{Eqn. (16)}$$

The parallel component of the gravitational force on the 50 lb load is given as follows:

$$F_{L,parallel} = F_{L} * \sin\theta \qquad \text{Eqn. (17)}$$

Summing forces gives an expression for the parallel component of the main pin reaction force:

$$F_{pin,parallel} = F_{L,parallel} - F_{act,parallel} \qquad \text{Eqn. (18)}$$

At a time of approximately 0.5 seconds when the bending stress is at a maximum, $F_{L,parallel}$ is equal to 23.2 lbs, $F_{act,\ parallel}$ is equal to 63.5 lbs, and $F_{pin,\ parallel}$ is equal to -40.2 lbs. This means that the section of the arm between the two pins is in tension, and the section between the actuator and the load is in compression. The compressive stress helps the principle stress level, while the tensile stress hurts it. Therefore, the tensile stress due to the section of the arm in tension was added to the maximum bending stress to calculate a maximum stress level in the worst possible case. Tensile stress due to an axial load is given as follows:

$$\sigma_{axial} = \frac{F}{A} \qquad \text{Eqn. (19)}$$

Where *F* is the axial force and *A* is the cross-sectional area. The axial force in the lower section of the arm, between the main pin and the actuator is 40.2 lbs. and the cross-sectional area is 0.9375 inches^2. This gives a tensile stress of 42.88 psi. This combines with the maximum bending stress of 884 psi to produce a maximum overall stress at the top outer fiber of the arm at the location of the actuator pivot of 926.88 psi.

Since this is a case where both loading conditions apply pure tensile stresses, the maximum von Mises equivalent stress is 926.88 psi. The tensile yield strength of sheet annealed 6061 aluminum is 8,000 psi (6), giving a static safety factor of 8.6 using the Distortion-Energy static failure theory.

With an arm geometry and material specification that provide an acceptable static safety factor against yielding, the slope and deflection diagrams were plotted using the singularity functions defined above. The deflection diagram shows a maximum deflection at the end of the arm of 0.008 inches, which is acceptable for this application.

This maximum deflection was then used to calculate the natural frequency of the arm. First, the spring rate of the arm was determined using the 44.37 lb. load which induced a deflection of 0.008 inches. This gave a spring rate of 5769.83 $\frac{lbs}{inch}$. The system mass is 50 lbs., or 0.129 blobs. The natural frequency of the arm is given by:

$$f_n = \frac{1}{2\pi}\sqrt{\frac{k}{m}} = 33.6\ Hz \qquad \text{Eqn. (20)}$$

This natural frequency is sufficiently high to prevent vibrations induced by a driving frequency of 10 Hz, the frequency of pressure pulses from the high speed on/off valve. Also of concern are the odd multiples of the 10 Hz driving frequency. While close to 30 Hz, the natural frequency of the arm is far enough away so it does not cause problems.

Rotation Calculations

The next step in the dynamic analysis of the mechanism was the calculation of the force required to rotate the mechanism. Figure 14 below serves as a key to define all the necessary geometric variables for the rotation of the mechanism.

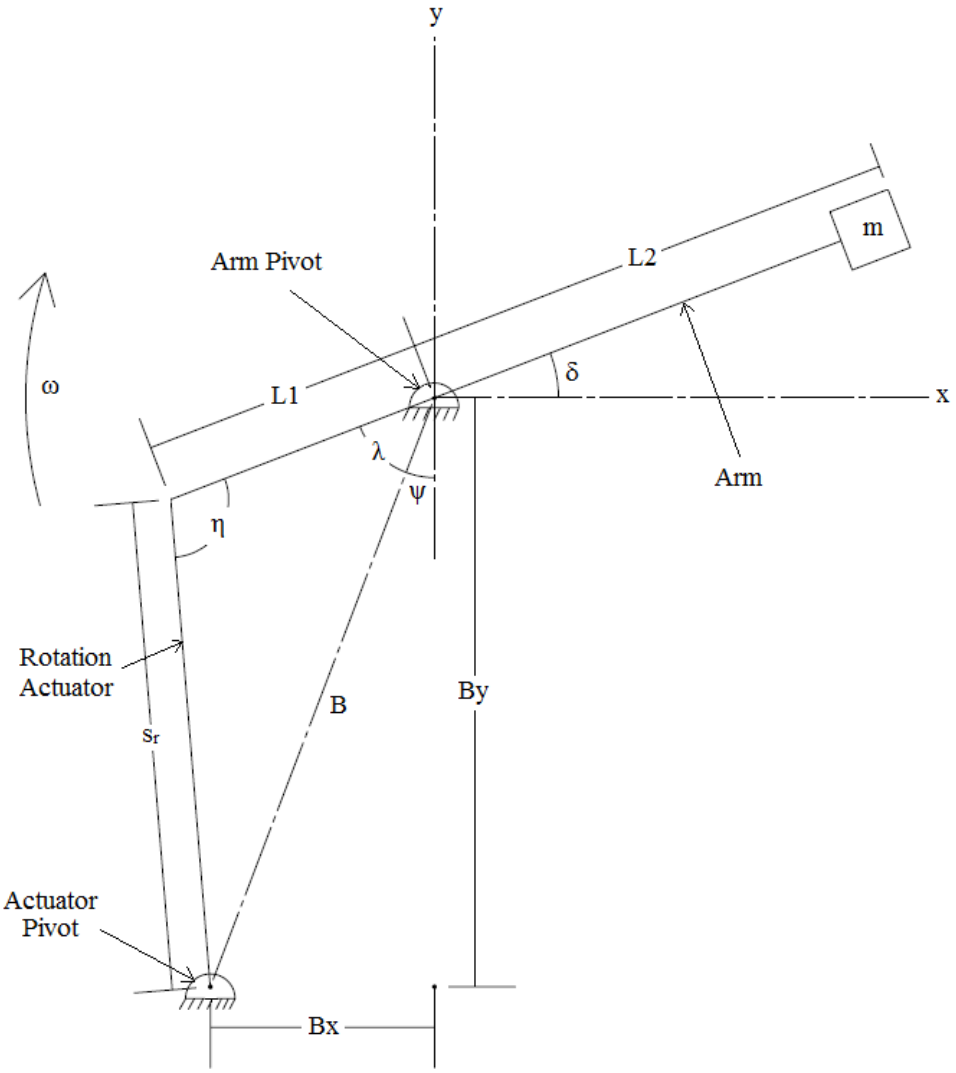

Figure 14: Rotation Variable Key

Similar to the variables defined in Figure 7 for the lift, *L1*, *L2*, *Bx*, *By*, and *m* are fixed values. The value s_r is the length of the rotation actuator, defined by the 3-4-5 polynomial function. η, δ, and λ are angles that vary with the length of the actuator. η and λ are both defined from geometry using the law of cosines. They are:

$$\eta = \cos^{-1}\left(\frac{B^2 + L1^2 - {s_r}^2}{2 * B * L1}\right) \qquad \text{Eqn. (21)}$$

$$\gamma = \cos^{-1}\left(\frac{{s_r}^2 + L1^2 - B^2}{2 * s_r * L1}\right) \qquad \text{Eqn. (22)}$$

Then from geometry, δ is defined as follows:

$$\theta = \frac{\pi}{2} - \lambda - \psi \qquad \text{Eqn. (23)}$$

This expression for the angular position was differentiated twice to obtain an expression for the angular acceleration of the arm during the two second rotation period. A plot of this function is shown below in Figure 15:

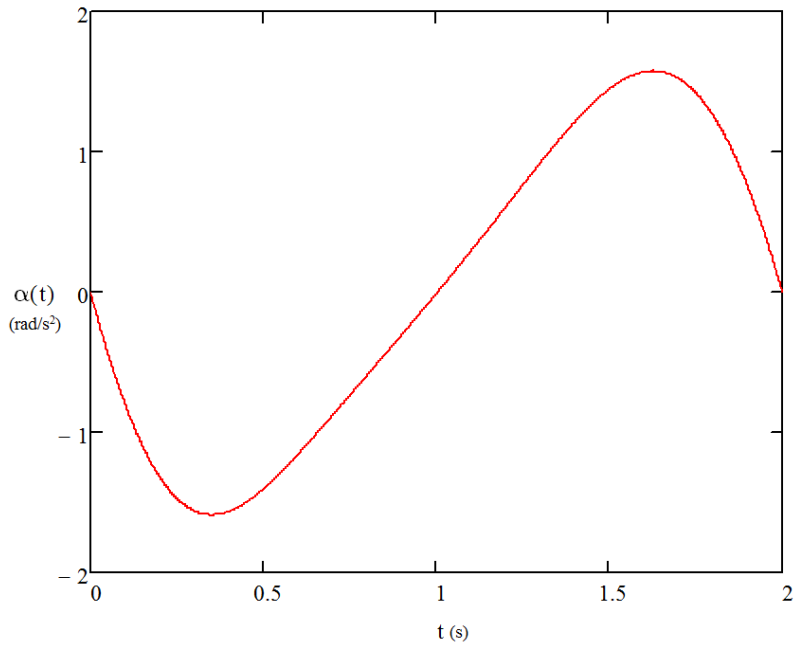

Figure 15: Rotation Angular Acceleration

To find the force needed in the actuator, Newton's second law was applied to determine the necessary torque to accelerate the mass at the rate specified in Figure 15. This relationship is as follows:

$$F_{act} = \frac{m * L2^2 * \alpha}{-L1 * \sin(\pi - \eta)} \qquad \text{Eqn. (24)}$$

Figure 16 below shows a plot of the required actuator force over the two second rotation period:

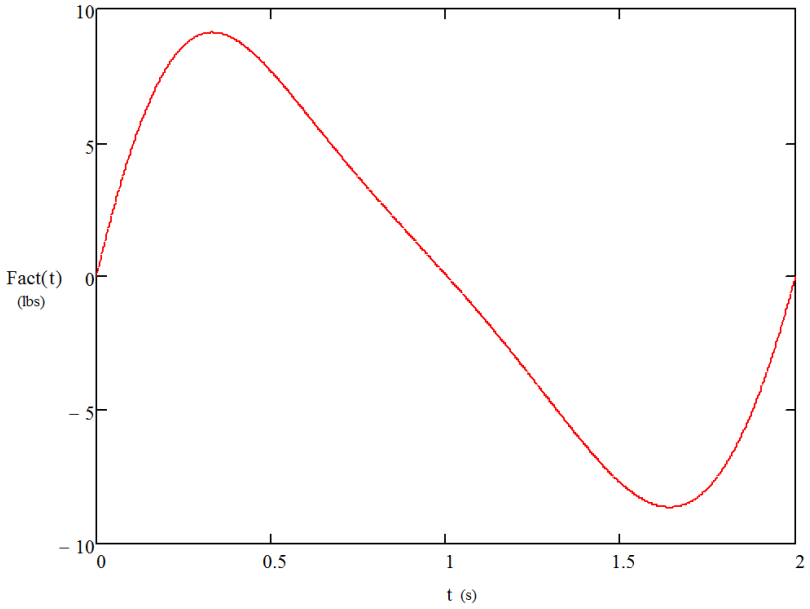

Figure 16: Rotation Actuator Force

Note that the required force from the rotation actuator is significantly lower than that required from the lift actuator, as seen in Figure 13. This translates to a low pressure requirement for the rotation relative to the lift, for a given cylinder area. Also note that the force required for the second half of the rotation is negative. As the arm is decelerating during this period, this negative force provides the opportunity for energy regeneration.

Additional Component Detail Design

In addition to the analysis performed on the arm, the shaft which supports the housing was also examined. This shaft was treated as a cantilever beam supporting a moment generated by the 50 lb. load and dynamic forces calculated above. The load is supported at a distance of 16 inches from the shaft, which therefore generates a moment at the root of the shaft of 800 in-lbs. A 20 mm shaft diameter was initially selected for its reasonable overall fit in the assembly. The maximum stress due to the bending moment was then calculated using the flexure formula. For a 20 mm shaft, the 800 in-lb. moment generates a maximum tensile stress of 16,691 psi. The most readily available steel alloy, 12L14, has tensile yield strength of 60,000 psi, giving a static safety factor for the shaft of 3.6. This confirms that the selected material and diameter is appropriate for the main shaft.

With a shaft diameter determined, it was also necessary to examine the loading on ball bearings sized for a 20 mm shaft. If traditional single row ball bearings had an unacceptably low life in this application, tapered roller bearings would be considered. In the case of this mechanism, the bearings are subjected to a combination of radial and thrust loads. The thrust load is simply the weight of the dumbbell load, or 50 lbs. The radial load on each bearing is determined by examining the moment applied by the dumbbell to the housing. The couple moment of the two bearings serves to counteract the load moment, as shown in Figure 17:

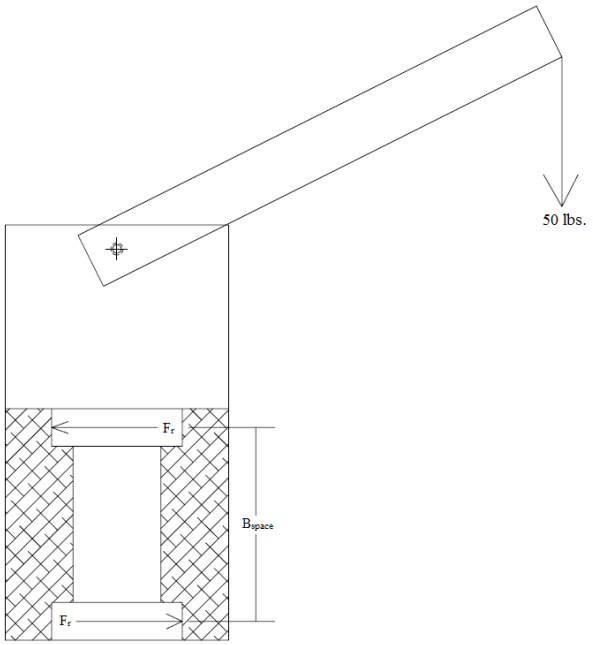

Figure 17: Free Body Diagram Showing Bearing Couple Moment

The moment applied by the load is again 50 lbs. at 16 inches, or 800 in-lbs. The radial load on each bearing is then:

$$F_r = \frac{M_{load}}{B_{space}} \qquad \text{Eqn. (25)}$$

Where B_{space} is the distance between the upper and lower bearings. For a spacing of 3 inches, this gives a radial load of 267 lbs.

Given both radial and thrust loads, an equivalent load, *P*, was calculated using equation 11.22a in Norton's *Machine Design* (6). This equation is as follows:

$$P = XVF_r + YF_a \qquad \text{Eqn. (26)}$$

Where F_r is the radial load, F_a is the thrust load, V is a rotation factor, X is a radial factor, and Y is a thrust factor. F_r and F_a were determined above from a static analysis of the system. V, X, and Y are calculated using Figure 11-24 in *Machine Design* (6). Relative to the load, the inner bearing race is rotating, so $V = 1$. 6304 bearings have a static load rating C_0 of 1,930 lbs., so the ratio $\frac{F_a}{C_0} = 0.026$. The factor e represents the minimum ratio between axial and radial loads below which axial load can be neglected. Interpolating in Figure 11-24, $e = 0.216$. The ratio $\frac{F_a}{F_r}$ is less than e, so $X = 1$, $Y = 0$. Therefore, the equivalent load, P, is equal to the radial load of 267 lbs.

The equivalent load was then used to calculate the L_{10} fatigue life of the bearings, the life before which 10% of a particular batch of bearings is expected to fail, expressed in millions of revolutions. For ball bearings, the L_{10} life is given by:

$$L_{10} = \left(\frac{C}{P}\right)^3 \qquad \text{Eqn. (27)}$$

C is the basic dynamic load rating, 3000 lbs. for a 6304 bearing. This gives an L_{10} life of 1418, or 1.4 billion revolutions. This ensures that there is very little change of 6304 bearings failing dynamically. Since the bearings are also loaded statically for the lift and lower portions of the mechanism's motion, the equivalent load, P, was also compared with the basic static load rating of the bearings. This static load rating, as stated above, is 1,930 lbs., giving a safety factor against static failure of 7.2.

Potentiometer Mounting Details

In order to properly control the motion of the arm during its lifting and rotating motions, it is necessary to monitor the position of the arm. Potentiometers were chosen as position-sensors for their relatively low cost and ease of integration into a control system. The hydraulic cylinders for the lift and rotation were purchased with position sensing magnets attached to their cylinders with the original intention of potentiometer sliders following these magnets as the cylinders extended. Preliminary testing revealed that the position sensing magnets were not strong enough to reliably carry a potentiometer slider.

Instead, a rotary potentiometer was attached to the main pin of the arm to sense the position during the lift, and a linear potentiometer was attached to the rotation cylinder, mechanically connected to the clevis at the end of the cylinder. To accommodate the rotary potentiometer, modifications were made to the arm, main pin, and housing. Instead of pressing

bushings into the arm and locking the pin to the housing, bushings were pressed into the housing. A setscrew in the arm locks the main pin to the arm, causing it to rotate as the arm is lifted. The shaft of the potentiometer is inserted into a hole in the end of the main pin, and a small setscrew locks it in place. The body of the potentiometer is then attached to the housing with a bracket. This arrangement is shown below in Figure 18:

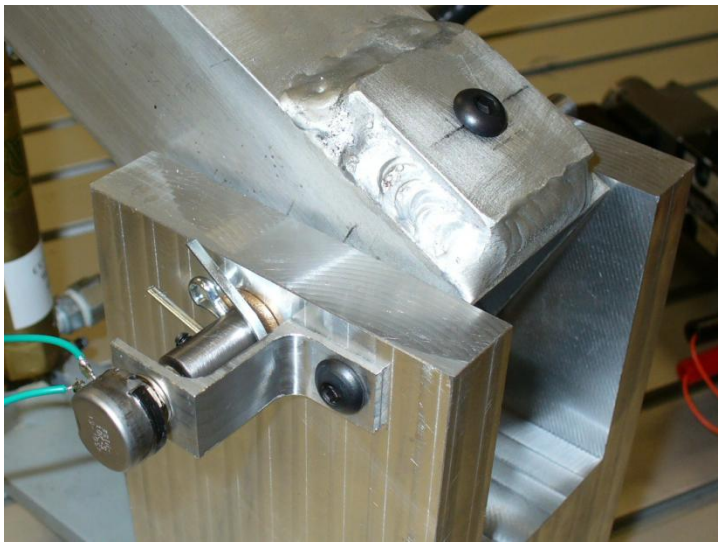

Figure 18: Rotary Potentiometer Mount

A similar scheme was devised to rigidly connect the slider of the linear potentiometer to the piston of the rotation actuator. In this case, a set of brackets clamps the body of the potentiometer to the cylinder body of the actuator. A link runs from the clevis at the end of the piston to the slider of the potentiometer, causing it to advance as the piston extends. This arrangement is shown below in Figure 19:

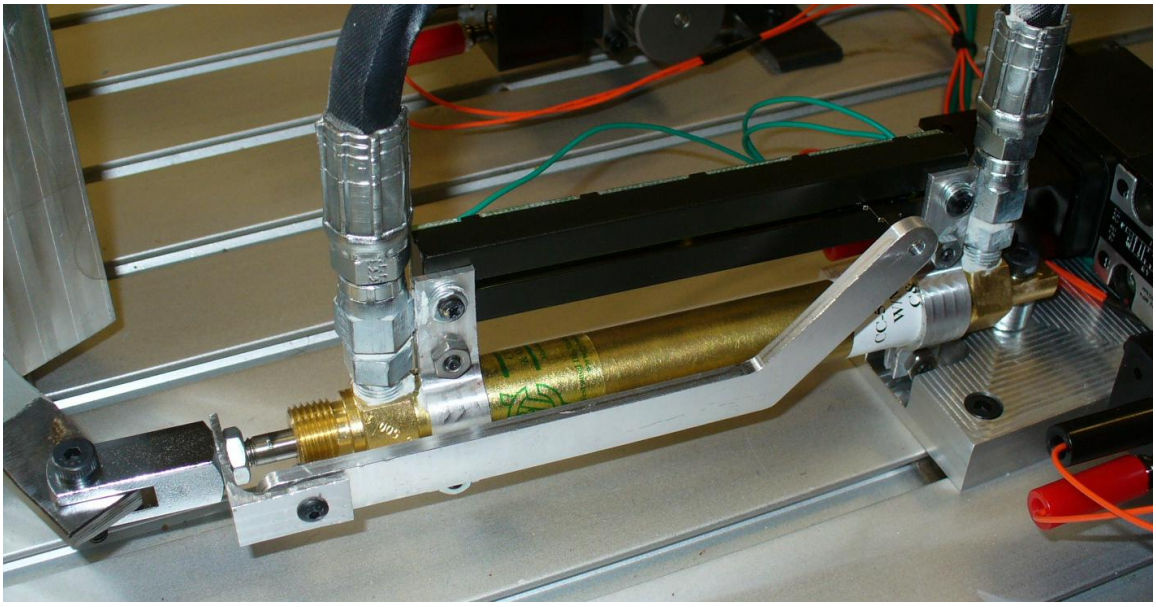

Figure 19: Linear Potentiometer Mount

Design of Hydraulic Circuit

In the multi-actuator switch mode hydraulic system used to drive the crane arm, a Festo fixed displacement pump is used to charge a one liter bladder style Festo hydraulic accumulator. Fluid is discharged from the accumulator and continues to the custom manifold which houses the high speed valve, DCV, and check valves. Fluid first flows to the Hydraforce 3-way solenoid high speed valve which switches at a constant frequency, sending pressure pulses through the rest of the system. Inserta check valves were installed within the manifold to control the pressure spikes caused by the pulses. The upper check valve allows flow from the outlet of the high speed valve to the accumulator, and blocks flow in the opposite direction. The lower check valve allows the actuator to draw flow from tank to maintain a steady pressure when the loaded arm is moving and the high speed valve is closed.

When the high speed valve is energized, it allows flow from the pump and the accumulator to the DCV. When the valve is de-energized, in the off state, flow is blocked by the valve. This allows time for the pump to charge the accumulator if needed. Additionally, inertia from the moving mass creates suction within the manifold channels. This suction force pulls fluid directly from tank and through the lower check valve to the DCV. This keeps the pressure in the actuator stable and allows the mass to continue its motion even when not getting flow from the accumulator.

From the high speed valve, fluid enters the DCV and is sent to either extend or retract the actuator depending on the DCV's state. The DCV has three states: open, closed, or crossed. When the DCV is open, fluid flows back into the manifold and out a side port to the cap end of the actuator, causing it to extend. When the DCV is in a closed state, the valve is blocked and no fluid will flow through it. When the DCV is crossed, fluid flows out the opposite side port of the manifold to the rod end of the cylinder, causing it to retract. As one end of the actuator is pressurized, causing the actuator to move, fluid from the other side is sent back from the actuator through the DCV and to tank. Figure 20 shows a schematic of this process below.

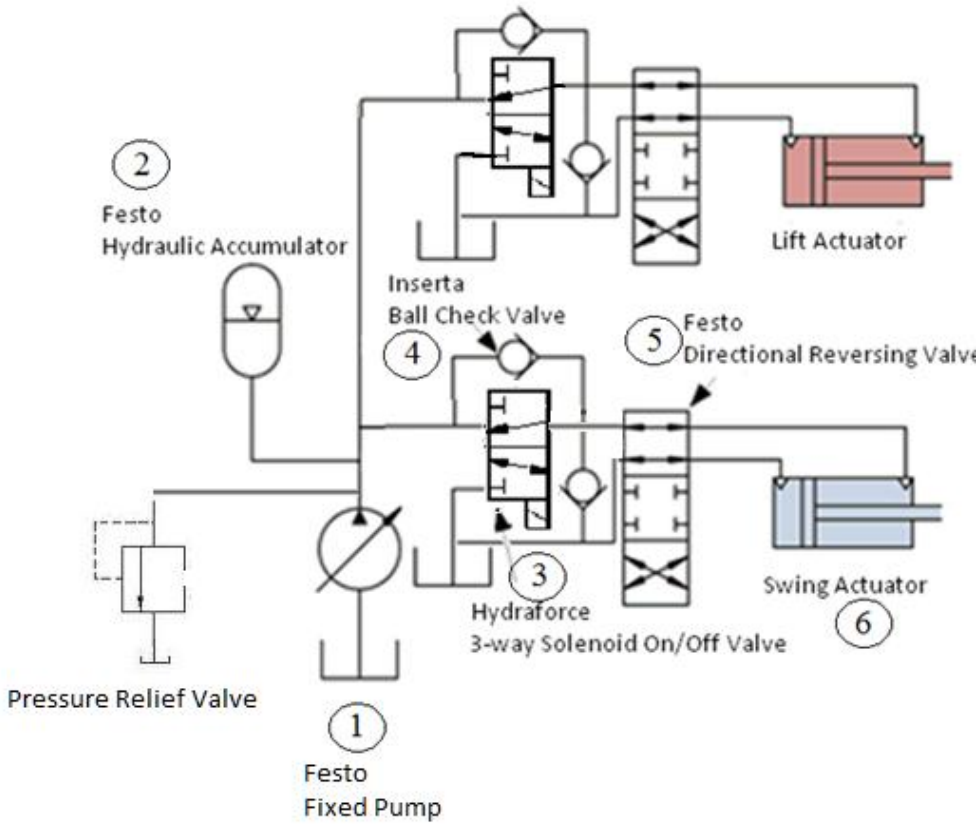

Figure 20: Multi-actuator Switch-mode Hydraulic Circuit

Manifold Construction

The manifold was constructed from a custom, 3" x 2 ¾" x 2 ⅛", 6061 aluminum block with drilled passages that connect various ports. It houses the on/off valve, the directional control valve, and two check valves shown in Figure 21 below. The main purpose of the manifold was to house these valves and reduce the need for an abundance of hoses. This keeps the hydraulic circuit neat and organized. As shown in Figure 21, ports for the pump and tank are on the manifold face closest to the variable displacement pump, making those hoses shorter and not interfering with other components in the system.

The top port of the high speed valve is needed to accept flow from the pump port and a check valve is needed to regulate the pressure between the top port and middle port of the high speed valve. This middle port then needs to allow flow from the high speed valve to the P port of the DCV. The ports directing flow from the DCV to the actuators are oriented on opposite faces of the manifold corresponding to the DCV state. For example, if the left side of the DCV were passing fluid, then the left face of the manifold would be the face allowing flow to the actuator.

The bottom check valve is placed between the middle port of the high speed and the tank port to allow flow to the system when needed. Plugs were placed in -4 O-ring boss ports above the check valves to seal the cavities. Since the T port of the DCV and the bottom port of the high speed valve both needed to flow to tank, one passage was designed to meet both needs.

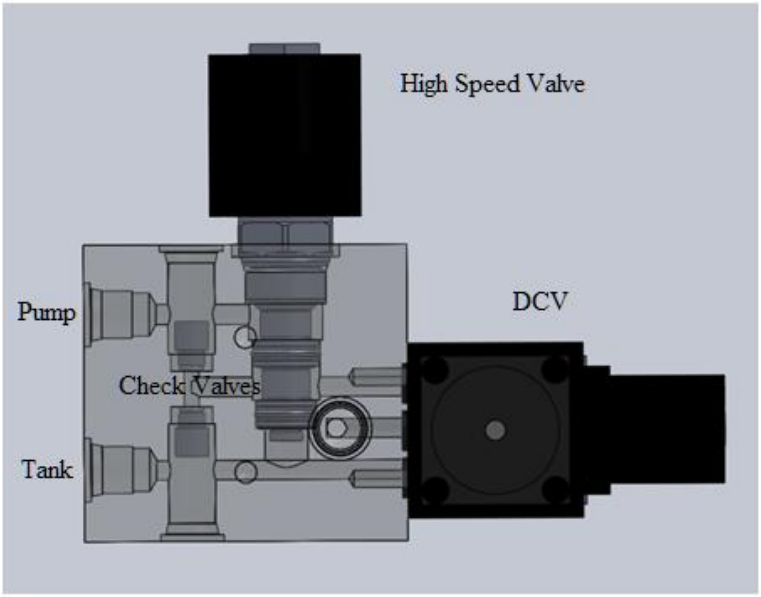

Figure 21: Skeletal View of Manifold with Valves

Several designs of the manifold were considered. Each iteration reduced the amount of material required and simplifying the geometry of the passages. Keeping manufacturing simplicity in mind, the final manifold design uses straight, 0.18" diameter passages; each entering the block perpendicular to the face. The passages were sized to the largest hole that would allow the required flow and velocity of fluid to the DCV without leakage. The ports connecting exterior hoses to the manifold were all -4 O-ring boss ports. To keep these ports consistent, a custom -4 O-ring boss port cutter was used. The manifold was mounted to the board using custom-sized L brackets. The manifolds were slightly elevated off the Festo mounting board to allow clearance for the plug used on the bottom face. The manifold design and orientation is shown in Figure 22 below.

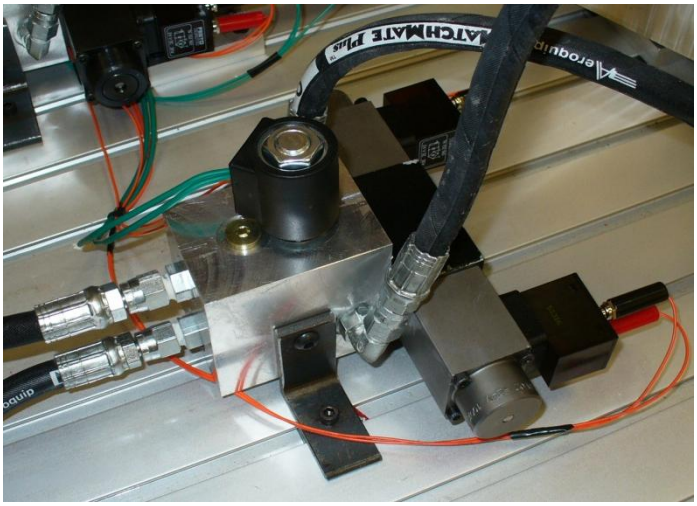

Figure 22: Manifold

Manifold Components

The Hydraforce SV08-30 solenoid on/off valve, seen in Figure 23, was chosen as the high speed valve. It was chosen because it meets the required 10 Hz switching frequency, has a response time of 20 milliseconds and a pressure loss of less than 10 psi. The valve neatly screws into the custom cavity machined into the manifold and seals with an O-ring.

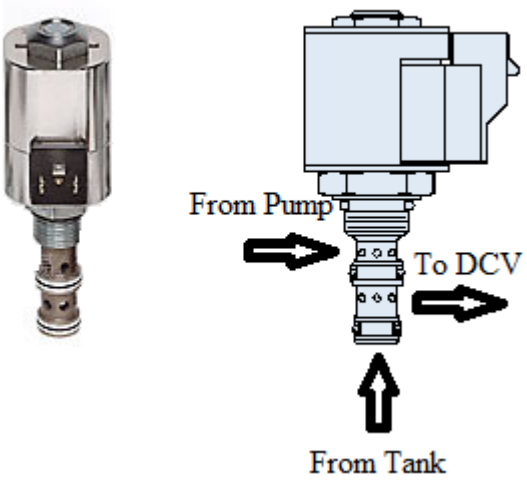

Figure 23: High Speed Valve with Flows: Hydraforce Catalog (7)

The directional control valve (DCV) used in the hydraulic circuit is a Festo Directional Control Valve. This was chosen because it was readily available in the MEPS lab and has the three states necessary to control the crane arm; open, crossed, and closed. The pressure loss

across the valve was also less than five psi, which was an acceptable loss for the valve. The Festo DCV is shown in Figure 24 below.

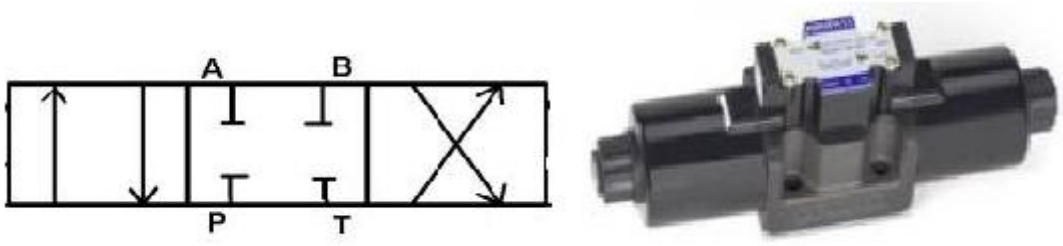

Figure 24: DCV with Schematic: Northeast Hydraulics (8)

The rotational actuator was the low pressure, high flow actuator. It required a maximum pressure 41 psi and maximum flow rate of 0.1912 GPM to rotate the crane arm. To find maximum pressure, the following equation was used:

$$P = \frac{F}{A} \qquad \text{Eqn. (28)}$$

$$P = \frac{8}{0.19635} = 40.7\ psi$$

Where *F* is the maximum force shown in Figure 16. *A* is the area at the cap end of the actuator. To find the maximum flow rate, the following equation was used:

$$Q = A * V \qquad \text{Eqn. (29)}$$

$$Q = 0.19635 * 3.75 = 0.1912 \text{ GPM}$$

Where *A* is the area at the cap end of the actuator and *V* is the maximum velocity of the rotational actuator.

The rotational actuator (gold) can be seen in Figure 19. The lift/lower actuator was the high pressure, low flow actuator. It required a maximum pressure of 305 psi and maximum flow rate of 0.086 GPM to lift the 50 lb. load attached to the arm. The flow was half of the required flow to rotate the crane arm. The lift/lower actuator is pictured below in Figure 25. To find maximum pressure, Eqn. (28) was used again:

$$P = \frac{134}{0.44179} = 303.95\ psi$$

Where *F* is the maximum force shown in Figure 13. A is the area at the cap end of the actuator.

To find the maximum flow rate, Eqn. (29) was used again:

$$Q = 0.3313 * .75 = 0.086\ GPM$$

Where *A* is the area at the cap end of the actuator and *V* is the maximum velocity of the rotational actuator.

Figure 25: Lift/Lower Actuator

Due to the fact that the greatest required pressure in the system is only 305 psi, the cracking pressure for the check valves was chosen to be three psi. An Inserta ball-type check valve, shown in Figure 26, was chosen to be used in the manifold. The model was selected because it was small enough to fit between the top and middle ports passages of the high speed valve. The valve also neatly screwed into its cavity, seating the o-ring on its bottom tightly to the bottom of the cavity. A custom tool was manufactured to tighten the valve into the manifold. A -4 O-ring boss port was machined into the top of the check valve cavity so a plug could be placed inside.

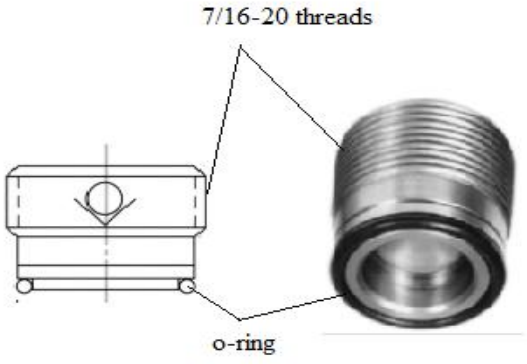

Figure 26: Inserta Thread-In Check Valve (9)

Circuit Layout

The circuit was constructed on a Festo Board that featured t-slots used to mount the components directly to the board. Attached above the board was the Festo fixed displacement pump used to power the system. The one liter bladder style Festo hydraulic accumulator was mounted directly to the Festo Board. The final circuit layout is shown in Figure 27 below.

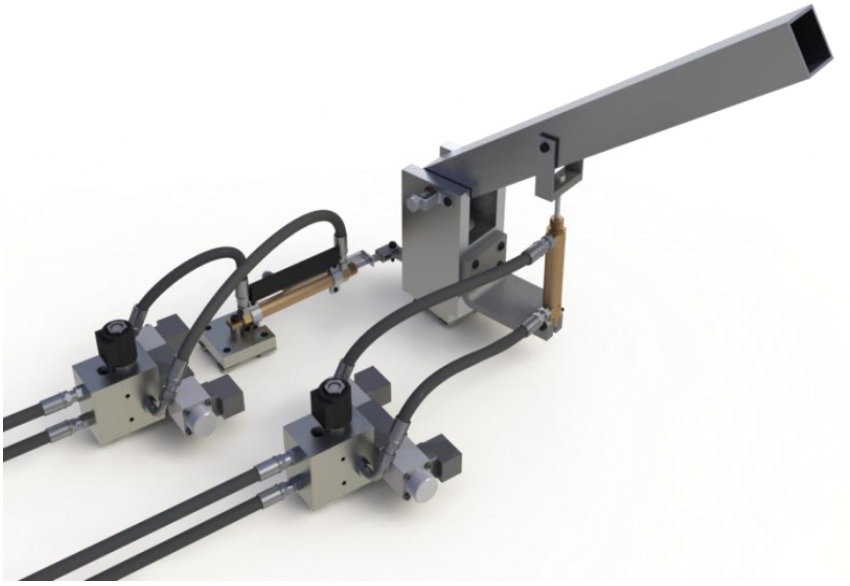

Figure 27: Multi-Actuator Switch-Mode Hydraulic Circuit

Design of the Control System

With both the mechanical crane arm and hydraulic circuit designed and in the process of being constructed, the team's focus shifted to the control system that would control the hydraulic circuit. The control system is comprised of two major components: a software component, LabVIEW, and a hardware component, the electrical circuit. These components were designed in unison with changes in one affecting the other. Prior to building an electric circuit the software component of the control system, LabVIEW, was addressed to define what parts would be required in the electrical circuit.

LabVIEW

The program LabVIEW was used to control the valves in the hydraulic system. The LabVIEW program, shown in Figure 28 below, reads in the theoretical position, defined by the 3-4-5 polynomial functions mentioned earlier, at discrete time steps. This theoretical position was compared with the actual position of the arm, read in from the DAQ board as voltages across the potentiometers. These voltages were converted to the extension length, for the linear potentiometer, and rotation angle, for the rotational potentiometer, by means of mathematical functions. Originally a PID block was going to be used to minimize error in the arm's actual position, but during testing it was discovered that the computer was unable to calculate the proportional, integral, and derivative gains fast enough for the system to run properly. Instead, the final program utilized a closed loop feedback system with only a proportional gain to amplify the difference between the theoretical and actual positions, representing the error in the system. The remainder of the programming in place was used to compensate for any errors by altering either the position of the directional control valves, or the duty cycle of the high speed valve. With the inputs and outputs of the control system defined by the software inputs and outputs in the LabVIEW program design and construction of the electrical circuit began.

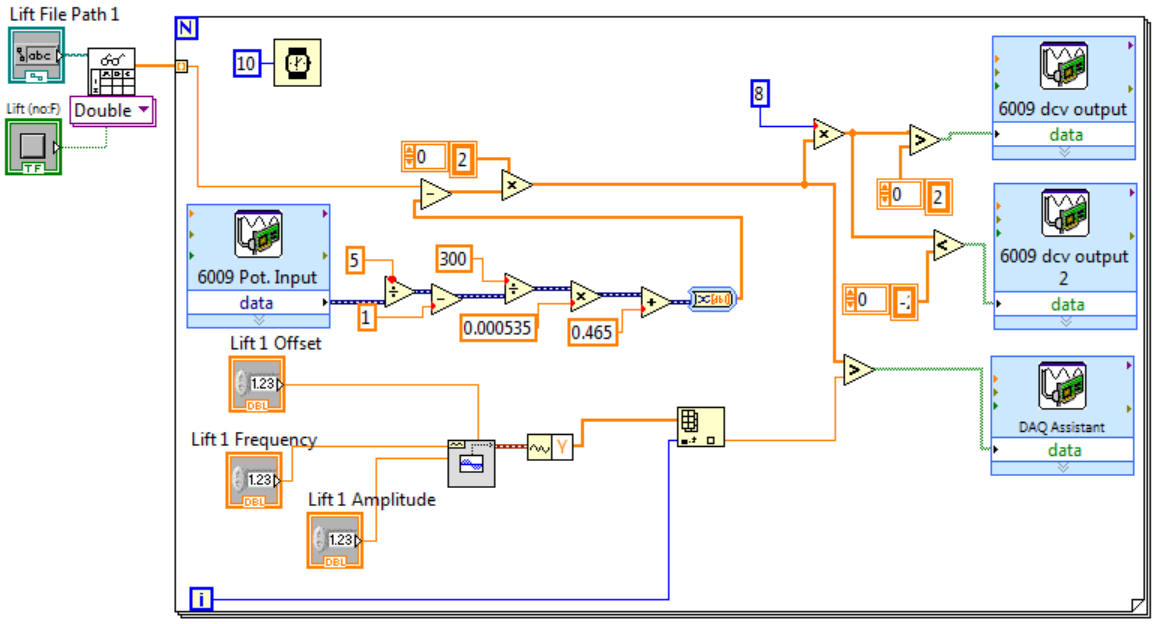

Figure 28: LabVIEW Lift Circuit

Electrical Circuit

An electrical circuit was designed around the control program written in LabVIEW. The directional control valves and the high speed valves in the system require 24 volts to operate. The DAQ board is only capable of outputting five volts, so an additional power source was required. The electrical circuit was constructed to provide this additional power to the required parts, to use transistors to connect and disconnect the individual components of the circuit, and to operate the high speed valve with a specified duty cycle. The circuit consists of a power supply, breadboard, rotary and linear potentiometers, transistors, and a USB 6009 DAQ board.

An Extech DC regulated power supply was selected for the circuit. The +24 volt variable output on the power supply was hard wired to one rail on the breadboard to supply the required 24 volts for the high speed valves and directional control valves, while the -24 volt variable output was wired to the common ground on the breadboard. Transistors were used as switches to activate each of these switches as designated by the LabVIEW code. The power supply also provided the five volts called for by the potentiometers by means of a hardwired five volt connection.

The rotary potentiometer has three connections: ground, power, and the wiper. To measure the voltage across the rotary potentiometer a voltage divider was needed because the range of motion of the rotary potentiometer in use was only ten degrees out of the 270 degrees of total rotation. Wiring a 300 Ω resistor in series with the rotary potentiometer increased the range of voltage drops across the potentiometer at its two extremes considerably. The downside to the voltage divider arrangement was the loss of linearity in the voltage readings. To compensate for this, the voltage divider equation shown below was used to solve for the resistance of the potentiometer given the voltage drop across it. This resistance was then filtered to produce an angular position. R_2 is the potentiometer resistance, R_1 is the fixed 300 Ω resistance, V_{in} is the input five volts, and V_{out} is the measured voltage across the potentiometer.

$$R_2 = \frac{R_1}{\left(\frac{V_{in}}{V_{out}} - 1\right)} \qquad \text{Eqn. (30)}$$

The power connection on the rotary potentiometer was connected to the DAQ board in series with the 300-Ω resistor, while the wiper was connected to the common ground on the breadboard.

The linear potentiometer has two separate potentiometers etched into the board, but the team only used one of them with its three connections: ground, power, and the wiper. The power was connected to the DAQ's five volt hardwired connection, and the ground was connected to the common ground on the breadboard. The wiper was connected directly to the DAQ's analog input channel to give a reading of the actual position of the hydraulic system in real time.

Each of the six TIP120 transistors, functioning as DC to DC power converters, was connected to ground, the 24 volt power rail on the breadboard, and the DAQ board. The transistor schematic is shown below as Figure 29. Two of the rails on either side of the breadboard are wired as common ground, while the other two rails are wired to power. One power rail to the five volt hardwired connection on the power supply, and the other to the variable 24 volt connection on the power supply. 1 kΩ resistors were used in series with each of the transistors to limit the amount of current drawn from the power supply. Even with the resistors in the circuit, when all of the transistors were active it was discovered that the power supply became current limited. Since the design never called for a situation in which all of the transistors are active at the same time, this was not perceived as a potential problem.

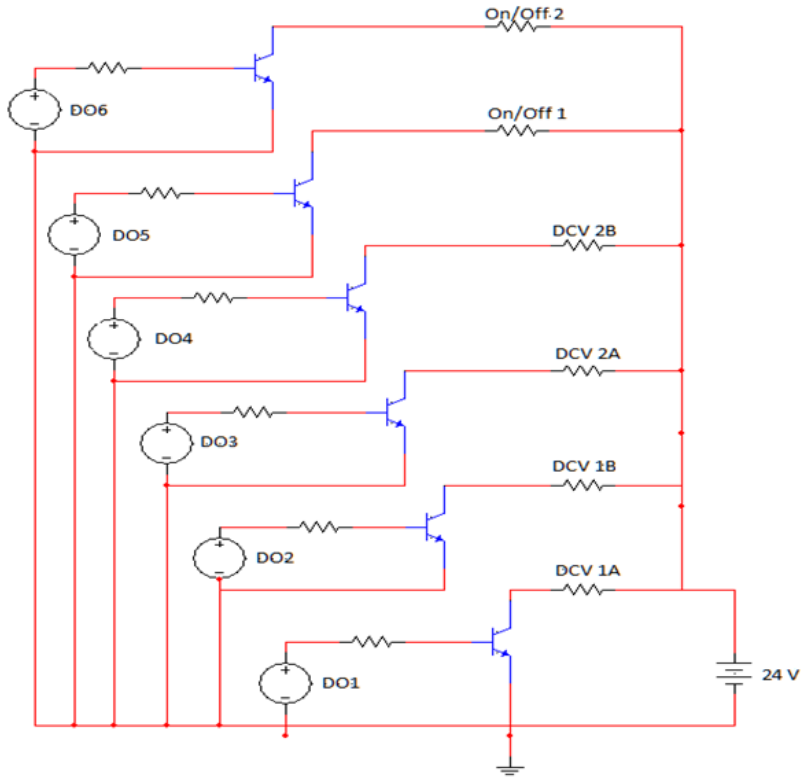

Figure 29: Valve Control Schematic

Results

Once all the pieces of the project came together, the control system was tested. First, each individual aspect of the system (lift, swing and lower) was tested. During this initial test, the high speed valve was set to the maximum duty cycle, meaning the pressure applied to the system by the accumulator was at its maximum. This essentially supplied a constant pressure and flow to the actuators to confirm that the mechanism would move through each phase as expected.

At this point in the testing process, it was observed that the system could not pressurize. It was determined that the system could not pressurize due to a design error in the manifold. As described in the manifold design section, two check valves were used to direct fluid flow. After inspecting the manifold it was apparent that the lower check valve was oriented upside down, causing fluid flow into the system to immediately loop back to tank. A quick fix to the problem was to remove the check valve and insert a setscrew to plug this passage. This allowed the system to fully pressurize and for testing of the system to continue.

With the system able to pressurize, the mechanism traveled through the entire range of motion as described in earlier sections, shown below as Figures 30 through 32. During the rotational motion the hoses connected to the lift actuator impeded the motion of the crane arm resulting in a higher pressure to swing the arm with the 50 lb. load attached than originally anticipated. This increased the required pressure to perform the rotating action, resulting in a high flow medium pressure component rather than the intended high flow low pressure. The only drawback from this unexpected force is the effect it would have on an efficiency analysis of the system. The reaction force to continually overcome the force from the hoses would decrease the amount of energy that the system could potentially capture as it re-pressurizes the accumulator.

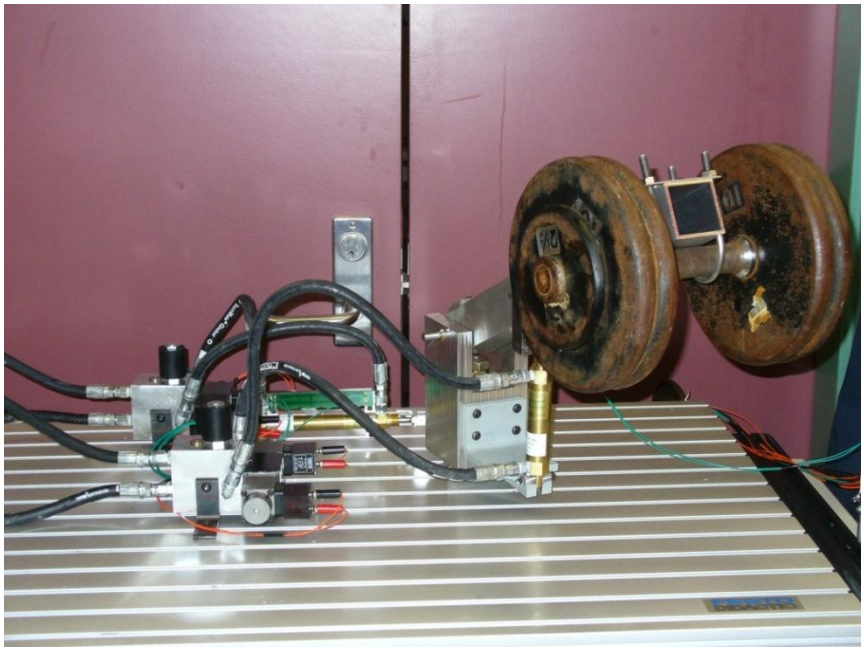

Figure 30: Mechanism Start

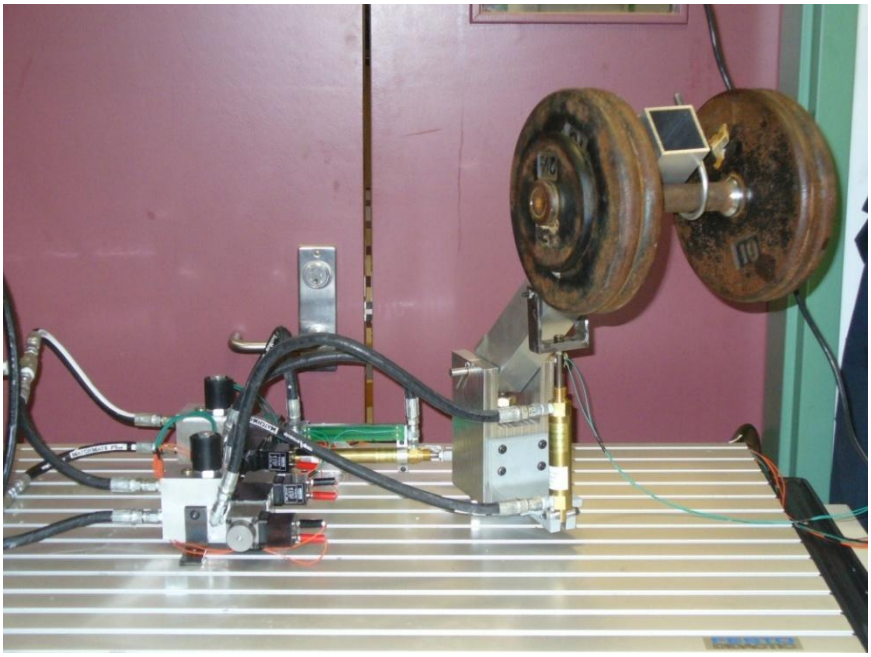

Figure 31: Mechanism Lift

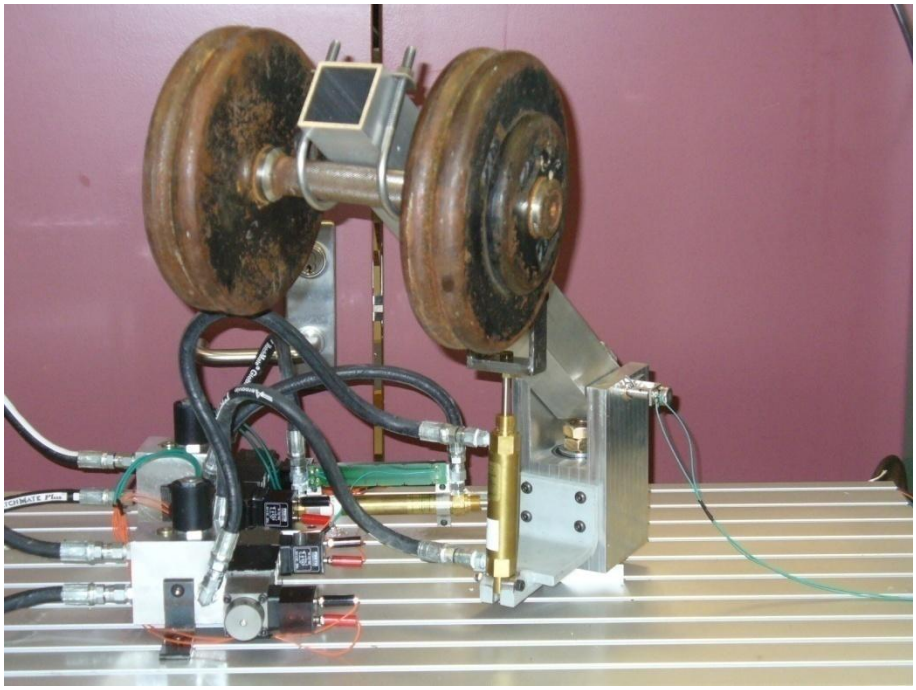

Figure 32: Mechanism Swing

The next step in the analysis process was to engage the high speed valve. With setscrews replacing the lower check valves in each manifold, fluid was unable to flow from tank and the suction created within the manifold worked to pull the moving mass back down. Now, the inertia created by the moving mass limited function of the system. As the inertia of the moving object increased, the suction within the manifold increased as well, creating cavitation within the manifold. This made testing the high speed valve with the 50 lb. weight attached impossible without re-machining the manifold blocks.

With time limited at this point in the project the team decided to maximize the smoothness of the crane arm's motion without an attached weight. The system pressure and control system inputs were optimized to create the smoothest motion of the mechanism possible.

Even though the system did not function as anticipated with the 50 lb. load, the fact that the mechanism was able to move at a considerably smooth rate proves that the theoretical technology does work experimentally. Video of the lift, swing, and lower operations were recorded and displayed during project presentation day, and was used to visually show that using switch-mode control can be used to create a smooth motion while generating energy savings in the system.

Discussion

Even a simply designed system utilizing switch-mode control technology requires multiple stages of testing to ensure that each element in the system is functioning correctly. As with many systems if a single part of the system fails or the response is uncharacteristic it can be troublesome to identify which part of the system is malfunctioning. To avoid this as much as possible the team did its best test in stages to make sure each piece of the system was working before moving on to the next component. Beginning with the most basic mechanical and hydraulic components the team worked their way through troubleshooting the system, and identifying potential problems as they arose.

During the first round of testing, prior to engaging the high speed valve in an oscillating function, the crane arm demonstrated its ability to lift, swing, and lower a 50 lb. dumbbell effectively. During the swing phase of the test the hoses connecting the lift actuator to the manifold greatly impeded the motion of the crane arm. This resulted in a medium pressure high flow situation that was not designed for. To correct this problem hoses with a larger radius could be attached, or the manifold could be mounted on top of a sliding mechanism to alleviate the added forces from the hydraulic hoses. The ability of the crane arm to withstand the forces on the mechanism with the 50 lb. dumbbell attached shows that the team's calculations for stresses were accurate. The hydraulic actuators also demonstrated their ability to lift and swing, which shows that the hydraulic calculations done to size both the actuators and accumulator were correct. During this stage it should be noted that the DAQ board was connected to read the voltage across the potentiometers and convert the voltage into actual position data. These key elements in the system needed to be done before engaging the high speed valve to ensure the safety of the group while operating the system. Had any of these parts of the system failed during the high speed valve testing there could have been a critical failure when the team did not have direct control of the pressure being applied to the system. A critical failure in this situation with the 50 lb. dumbbell attached to the arm could have resulted in the load being thrown or dropped outside of the test area. With both the hydraulic and mechanical systems tested for safety, further testing of the system could commence without fear of a critical failure in the system.

The second round of testing began by engaging the high speed valve. At this point in the testing process the team encountered numerous problems with the LabVIEW programming, which started by trying to enable the high speed valve and getting no response. These problems were eventually resolved, but this delayed testing and resulted in the PID block being removed from the LabVIEW program completely. The PID block was replaced with simpler proportional gain control within the closed loop feedback system. Once the programming allowed the high speed valve to be enabled with a frequency of 10 Hz testing resumed. The new response from this round of testing was noticeably different from the previous tests. The arm could no longer generate enough pressure to lift the crane arm with a weight attached. After further troubleshooting with the LabVIEW programming it was determined that the program was functioning correctly and the problem was with the design of the manifold. One of the check valves inside the manifold that was supposed to enable flow to come from tank was designed and installed upside down. Without the ability to pull fluid from tank, the system would be unable to lift any load due to cavitation occurring inside the manifold block when the high speed valve was in the "off" position and the crane arm was attempting to lift a load. This error also prevented the team from doing proper efficiency calculations as the main form of energy savings was disabled in the system.

With the manifold unable to pull flow from tank, efficiency experiments could not be conducted effectively, so the team decided to make the most of the situation and continue on with testing that was still possible. Using LabVIEW the team optimized the performance of the system, so the effectiveness of the 10 Hz switching frequency could be determined by visual inspection in comparison with classic throttling technology. Without pulling flow from tank, the smoothness was less than it could have been. The motion was still consistent and fairly smooth. The lift, swing, and lower motions were recorded on video, and show that this theoretical technology can be implemented in a hydraulic system.

Using switch-mode control with a 10 Hz oscillating valve is restricted by the jerk of the mechanism from the pressure pulses. It was seen experimentally that the limiting element in the switch-mode control is indeed the off-the-shelf 10 Hz valve. Even with this mechanical limitation, the system did function with a smooth enough motion to call the system functional. When comparing the motion of the crane arm operating with switch-mode control to that of a "wide open" throttle the motion is noticeably jerkier. With the future implementation of a 100

Hz frequency valve currently being developed by Professor Van de Ven in the MEPS lab, the switch-mode control would smooth out even further and have more implementation possibilities, especially when combined with a fully functional manifold block.

Conclusions

The purpose of this project was to implement switch-mode control in a multi-actuator circuit and demonstrate the improvement in this system's efficiency over a traditional hydraulic system. With the designed system limited in its ability to demonstrate the efficiency of the switch-mode technology, verifying a smooth output motion through the lift, swing and lower demonstrates the potential capability of this emerging technology. Testing on the crane arm was performed on the order of 200 psi with valves and hoses rated for up to 3,000 psi. This means that the design detailed in this report could be scaled up significantly to 2,000 to 3,000 psi before requiring the significant redesign of many of the components in the system.

The testing platform developed to experimentally test this theoretical technology successfully demonstrated the function of switch-mode technology by performing the lift, rotation, and lower applications with a smooth motion. The motion demonstrated by this project will improve significantly once the 100 Hz high speed valve, currently being developed by Professor Van de Ven at Worcester Polytechnic Institute, is installed.

While the testing platform does demonstrate the ability of switch-mode control to function, the inability of the system to lift a 50 lb. weight as designed was disappointing. With cavitation occurring within the manifold due to the setscrew blocking the path for fluid to flow from tank, lifting a load cannot be accomplished until the manifold is redesigned with the bottom check valve installed so that fluid can flow from tank.

In the future, switch-mode control could be implemented in almost all multiple actuator hydraulic applications to improve efficiency. Current hydraulic systems, like the backhoe example in the introduction, could implement this technology to reduce the total required flow that must be generated by the pump, and therefore greatly increase the total efficiency of the entire system. Even more exciting, is the possibility of implementing switch-mode control in hybrid vehicles where each tire is controlled by a hydraulic motor. This would not only be advantageous for technologies like traction control, or ABS, but also for regenerative braking where energy typically lost as heat could be recaptured through the re-pressurization of accumulators in the hydraulic system.

Multi-actuator switch-mode hydraulic systems have a bright future, and with continued testing and experimentation, this technology will continue to grow and one day find itself at the forefront of the fluid power industry.

References

[1] Cundiff, John S.*Fluid Power Circuits and Controls: Fundamentals and Applications.* Boca Raton, FL : CRC Press, 2002. 0-8493-0924-7.

[2] *Switch-Mode Hydraulic Circuit for EOD Robot Manipulator.* Van De Ven, James D. 1, 2010.

[3] Van Den Brink, R. "The Axial Piston Pump with Variable Displacement." 23 July 2009. Web. 28 Apr. 2011. http://home.planet.nl/~brink494/axpp_v_e.htm.

[4] *Design of a High-Speed On-Off Valve.* Van De Ven, James D. 2009.

[5] Norton, Robert L. *Design of Machinery*. New York, New York: McGraw-Hill, 2008. Print.

[6] Norton, Robert L. *Machine Design: An Integrated Approach.*" Boston: Prentice Hall, 2006. Print.

[7] SV08-30 Spool, 3 Way. Hydraforce Catalog. Pgs 1.300.1-1.300.2.

[8] Hydraulic Directional Control Valves. Northeast Hydraulics, Inc. 2011. http://www.northeasthydraulics.com/hydraulic-directional-control-valves.html.

[9] Thread-in Check valves. Inserta Catalog. Pgs 16-17.